An Integrated Battery Charger for EVs Based on a Symmetrical Six-Phase Machine

I. Subotic, E. Levi
Liverpool John Moores University, Liverpool L3 3AF, U.K.
i.subotic@2011.ljmu.ac.uk, e.levi@ljmu.ac.uk

***Abstract*−A new topology for integrated on-board battery charging is proposed in this paper. A symmetrical six-phase machine and inverter, which are used for propulsion, are incorporated into the charging process. The configuration achieves power transfer through the machine without developing an average torque in it during the charging mode. Additional degrees of freedom of six-phase machines are explained and it is shown how they can be utilized to transfer a part of the excitation from the torque producing plane into the non-flux/torque producing plane of the machine, so that rotation does not take place. The advantage is that the motor does not have to be mechanically locked during the charging process. The configuration is operated with a unity power factor and the appropriate control scheme is introduced for this purpose. Theoretical considerations are validated by simulations for both charging and vehicle-to-grid (V2G) modes of operation.**

I. Introduction

A standard solution in automotive industry nowadays is the use of an on-board charger that is placed in a vehicle as a separate unit. Since it does not use the existing power electronics components, it is usually called non-integrated charger. This charger contains additional components, and, when placed on-board, it contributes to the increase in weight, and decrease of the spare space in the vehicle. However, the main power electronics elements that a non-integrated charger requires already exist on-board: these are predominantly in the form of a voltage source converter (VSC) and filtering inductances. A VSC can be found on-board in all EVs with ac propulsion motors, since it is needed to produce ac voltages for supplying the motor from the battery (when operated in the inverting mode). The role of filtering inductances can be taken up by the stator windings of the electric motor. Thus, if these existing elements are reused in the charging process, savings could be remarkable.

It is shown in [1] that induction and permanent magnet motors are the preferred types of propulsion machines in vast majority of EVs. For these types of machines a several single-phase integrated topologies have been suggested. However, single phase charging is slow and hence time consuming. In order to achieve a fast charging process, either a dc charging station or a three-phase ac grid have to be used. In the case of the former possibility a driver depends heavily on the dc charging stations' distribution, and has to plan the route according to their disposition. In contrast to the dc charging stations, three-phase grid is widely available. However, there are relatively few solutions that enable integrated fast charging with induction and synchronous propulsion motors [2-9]. In some of the schemes there is the torque production in the machine during the charging process, so that the rotor of the machine has to be mechanically locked during charging. This causes lower efficiency, noise, and increased wear. Only four of the available configurations are viable for machines of induction or permanent magnet type if torque-free operation during the three-phase charging process is mandatory [6-9].

A three-phase machine in an open winding configuration, supplied from a triple H-bridge inverter, is integrated in the charging process in [6]. In the charging mode the three-phase grid is connected directly to mid-points of each of three machine's stator phase windings. The charging process is realised in such a way that the same currents flow through the two half-windings of each phase, where the half-windings are in spatial opposition so that the winding does not produce a field in the rotor. However, the machine has to be custom made to have access to stator phase winding mid-points – in essence it has to be a symmetrical six-phase machine. The advantage of the configuration is that the same topology is used both for charging and for propulsion without any hardware reconfiguration between the operating modes.

Another configuration that does not require any hardware reconfiguration is introduced in [7]. It incorporates a nine-phase machine with three isolated neutral points into the charging process. In the charging mode the three grid connections are directly connected to the three isolated neutral points of the machine. The topology is controlled in such a way that the same currents flow through all windings belonging to the same three-phase set, so that the field is cancelled within the set itself.

The first fast integrated charging topology that found its way into the industry is the one used in Renault ZOE [8]. Its 43kW "Chameleon" charger can charge 80% of the battery capacity in thirty minutes. The inverter and the synchronous motor with excitation winding, which are used for propulsion, are integrated into the charging process. In addition to these components the charger has a junction box which is a non-integrated element. It is used to manage the charging process, to convert the alternating current into the direct current (thus requiring additional power electronics) and to communicate with the charging station. There is no torque production in the machine during the charging process.

Finally, a configuration based on an asymmetrical six-phase machine is considered in [9]. The phase transposition [10] principle is employed to ensure torque-free operation during the charging process.

In this paper, a symmetrical six-phase machine and a six-phase inverter are incorporated into the charging process. A six-phase machine is considered due to its fault-tolerant properties in the propulsion mode, since it can continue to

Pre-print. Final version of this paper appears in IEEE Xplore Digital Library (http://ieeexplore.ieee.org/Xplore/guesthome.jsp).

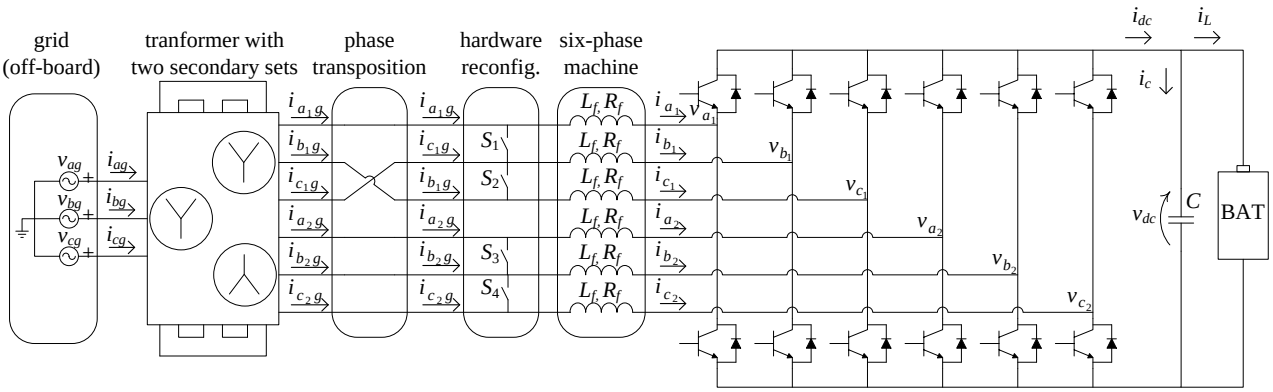

Fig. 1. Topology of the symmetrical six-phase integrated battery charging system. The transformer is assumed to be situated off-board, in the charging station.

operate with a rotating field as long as there are at least three healthy phases. The main advantage of this configuration relates to the charging mode, since a symmetrical six-phase machine has more degrees of freedom than a three-phase machine [11]. It is shown here how these additional degrees of freedom can be used to achieve charging through machine's stator windings without an average torque production in the machine.

The paper is organised as follows. In section II theoretical analysis is provided for a symmetrical six-phase charging system. In section III a mathematical model of the VSC is given, and the control algorithm for the charging mode is discussed. Theoretical results are verified by simulations in section IV. Section V outlines conclusions of the paper.

II. Operating Principles of a Symmetrical Six-Phase Charging System

It is shown in [9] how an asymmetrical six-phase machine can be used as a fast battery charger for EVs. Here a configuration that incorporates a symmetrical six-phase machine, operated with two isolated neutral points in propulsion mode, is considered for the same application.

In the charging mode it is necessary to open the machine's neutral points and to put the stator phases into an open-end winding configuration. A transformer with two star-connected secondaries (with outputs shifted by 180°) provides a symmetrical six-phase voltage system (off-board), which is connected to the stator winding (Fig. 1). However, the supply is not connected in the same sequence as to match phase order of the machine (phases a_{1g}-c_{2g} of the supply to phases a_1-c_2 of the machine). Instead, the idea of phase transposition [10, 12] is used to ensure a torque-free operation. This comes down here to transferring a part of excitation from the flux/torque producing plane into the non-flux/torque producing plane (x-y). The required phase transposition, which enables achieving the stated goal of torque-free charging, is illustrated in Fig. 1.

The decoupling transformation matrix for the symmetrical six-phase system is well known and can also be obtained from the general decoupling matrix for multiphase systems [11]. For theoretical analysis, it is beneficial to combine pairs of rows in 2D space vectors, which can be formulated as (f stands for any variable that is being transformed, e.g. voltage, current, etc.; α–β and x–y indices denote axis components):

$$\begin{aligned}\underline{f}_{\alpha\beta} &= \sqrt{2/6}\,(f_{a_1} + \underline{a}^2 f_{b_1} + \underline{a}^4 f_{c_1} + \\ &\quad + \underline{a}^1 f_{a_2} + \underline{a}^3 f_{b_2} + \underline{a}^5 f_{c_2}) \\ \underline{f}_{xy} &= \sqrt{2/6}\,(f_{a_1} + \underline{a}^4 f_{b_1} + \underline{a}^8 f_{c_1} + \\ &\quad + \underline{a}^2 f_{a_2} + \underline{a}^6 f_{b_2} + \underline{a}^{10} f_{c_2})\end{aligned} \tag{1}$$

where $\underline{a} = \exp(j\delta) = \cos\delta + j\sin\delta$ and $\delta = 2\pi/6$.

The six-phase supply currents for charging mode are:

$$\begin{aligned} i_{a_1 g} &= \sqrt{2} I \cos(\omega t) & i_{b_1 g} &= \sqrt{2} I \cos(\omega t - 2\pi/3) \\ i_{c_1 g} &= \sqrt{2} I \cos(\omega t - 4\pi/3) & i_{a_2 g} &= \sqrt{2} I \cos(\omega t - \pi/3) \\ i_{b_2 g} &= \sqrt{2} I \cos(\omega t - 3\pi/3) & i_{c_2 g} &= \sqrt{2} I \cos(\omega t - 5\pi/3) \end{aligned} \tag{2}$$

According to Fig. 1, the relationship between machine phase currents and supply phase currents is given with the following equations:

$$\begin{aligned} i_{a_1} &= i_{a_1 g} & i_{b_1} &= i_{c_1 g} & i_{c_1} &= i_{b_1 g} \\ i_{a_2} &= i_{a_2 g} & i_{b_2} &= i_{b_2 g} & i_{c_2} &= i_{c_2 g} \end{aligned} \tag{3}$$

Using (1) in conjunction with (2)-(3), the following is obtained for the machine's two current space vectors:

$$\underline{i}_{\alpha\beta} = \sqrt{6} I \cos(\omega t) \tag{4}$$

$$\underline{i}_{xy} = j\sqrt{6} I \sin(\omega t) \tag{5}$$

It follows that the flux/torque producing plane is excited, but only the α component exists; thus the field will be pulsating. It is known that only a rotating field can produce a starting torque in the machine; a pulsating field is not capable of producing an average torque, thus the machine will stay at standstill even without a mechanically locked rotor. From (5) it can be seen that only the y component of the x-y plane is excited, which is expected because it complements the α component to produce overall phase currents that will charge the battery. Zero-sequence components are both equal to zero.

III. Control of the Six-Phase Voltage Source Rectifier

Modelling and control of three-phase VSCs in rectification mode (VSRs further on) can nowadays be regarded as well-known, and their mathematical model is widely available (see

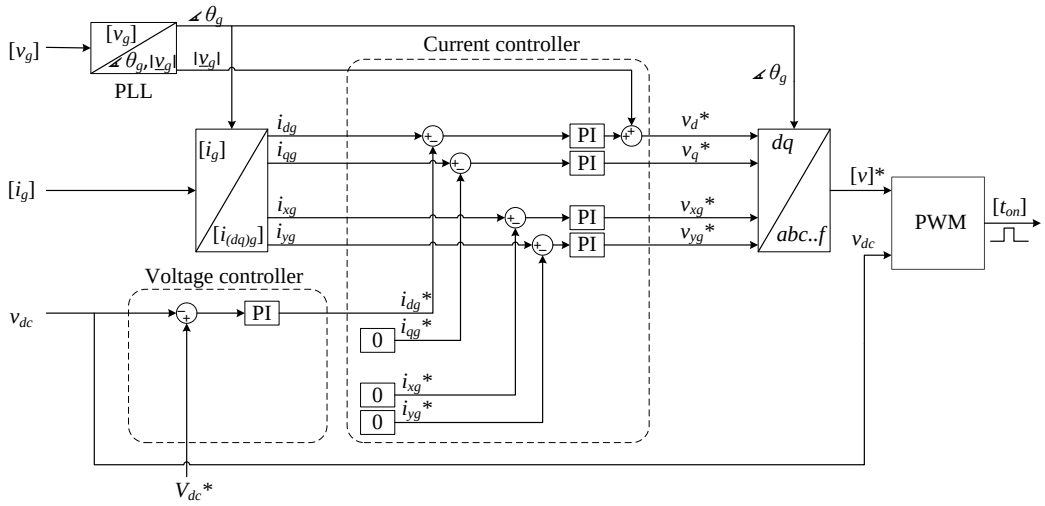

Fig. 2. Controller structure for the charging process.

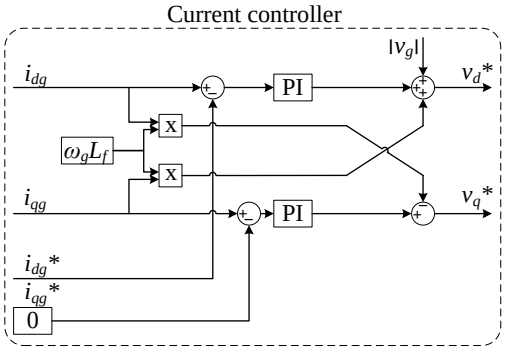

Fig. 3. Decoupling network.

[13], for example). On the other hand, multiphase rectifiers have not attracted much attention in the past, since there are not many real-world applications that demand this type of rectifiers.

A suitable mathematical model of a multiphase VSR with an odd number of phases, in the synchronously rotating reference frame, has been introduced recently in [5]. For an even number of phases the form is slightly different, as given in [9]:

$$\left[v_{g(dq)}\right] = L_f \frac{d\left[i_{g(dq)}\right]}{dt} - L_f \begin{bmatrix} 0 & \omega_g & 0 & \dots & 0 \\ -\omega_g & 0 & 0 & \cdots & 0 \\ 0 & 0 & 0 & \cdots & 0 \\ \vdots & \vdots & \vdots & \ddots & \vdots \\ 0 & 0 & 0 & \dots & 0 \end{bmatrix} \cdot \left[i_{g(dq)}\right] +$$

$$+ R_f \left[i_{g(dq)}\right] + v_{dc} \cdot \left([I]_{n\times n} - \begin{bmatrix} [0]_{(n-2)\times(n-2)} & \begin{matrix} 0 & 0 \\ \vdots & \vdots \end{matrix} \\ \begin{matrix} 0 & \dots \\ 0 & \dots \end{matrix} & \begin{matrix} 1 & 0 \\ 0 & 0 \end{matrix} \end{bmatrix}_{n\times n} \right) \left[s_{(dq)}\right] \quad (6)$$

$$C\frac{dv_{dc}}{dt} = [s_{(dq)}]^T \cdot [i_{g(dq)}] - i_L \quad (7)$$

where $[v_{g(dq)}]$ is the supply (six-phase grid) phase voltage matrix, $[i_{g(dq)}]$ the grid phase current matrix, and $[s_{(dq)}]$ the matrix of switching states, all in the rotating reference frame.

In order to achieve the unity power factor operation, grid voltage orientation is used for control (VOC). Measurements are required for six-phase grid phase voltages, dc-bus voltage, and grid currents.

At first the grid position is obtained, using a phase-locked loop (PLL). The grid position is used to transform grid currents into the reference system that is grid voltage oriented. This means that the grid current component that is in phase with the grid voltage will become a dc quantity. If the charging process utilizes only this component that is in phase with the grid voltage, the unity power factor will be achieved. This dc component can be controlled with a simple PI controller. However, there is also the *q*-axis component and two additional components in the second plane (*x* and *y*). They are all also dc quantities, so that they can be controlled with PI controllers as well. The *q*-axis component is not in phase with the grid voltage; hence it should be controlled to zero. The *x*-*y* components of the second plane only contribute to losses; thus they should be controlled to zero as well. The control of these components in the second plane is the only difference with regard to a three-phase VSR system control. The complete VOC diagram is presented in Fig. 2.

If the charger is operated in the constant current (CC) mode, than the input reference to the system is just the desired value of the grid current *d*-axis component. If it is operated in constant voltage (CV) mode, the reference is the dc-bus voltage. The difference between a battery voltage and a dc-bus voltage is directly proportional to the battery charging current, thus the reference for the *d*-axis component of the current is obtained by a PI voltage controller which is presented as the outer control loop in Fig. 2.

It can be seen from (6) that *d*-*q* current components are not decoupled, so that the change of one component causes a change in the other one as well. Thus a decoupling network is required between these two components, which is for clarity reasons not included in Fig. 2 and is presented separately in Fig. 3 instead.

As the modulation technique, a simple carrier based PWM with zero-sequence injection is utilized. However, due to the existence of two isolated (by transformer) sets of three-phase

systems (a_1-b_1-c_1 and a_2-b_2-c_2) zero-sequence current cannot flow between sets; it is thus possible to utilise the standard three-phase zero-sequence injection in the PWM process. The advantage is the lower dc-bus voltage requirement (for the same performance), which is in essence equal to the value that is needed for the three-phase system.

The control diagram, shown in Fig. 2, is also valid for the vehicle-to-grid (V2G) operation. The only difference is that in the constant current (CC) mode the *d*-axis current component reference should be set to a negative value to obtain grid currents that are in phase opposition with the grid voltages. If the converter is operated in constant voltage (CV) mode the dc-bus voltage reference should be set to be lower than the battery voltage to achieve the V2G operation. Apart from the change in the reference, no other modifications of the control diagram are necessary for the change between the modes of operation (charging/V2G).

In the propulsion mode the drive is operated according to the field oriented control (FOC). This mode of operation is well covered for multiphase machines and will not be considered here.

IV. Simulation Results

To verify theoretical principles, simulations of the symmetrical six-phase charging/V2G system are performed in Matlab/SimPowerSystems environment. A symmetrical six-phase grid, obtained as shown in Fig. 1, is assumed to be available. It is of 240V_{rms}, 50Hz frequency, and the voltages are assumed to be perfect sine waves. Converter switches at 10kHz, and the dead-time effect is neglected. The dc-bus capacitance is taken as 1.5mF. Battery is modelled as a simple resistor of value R_L=0.5Ω, in conjunction with an ideal voltage source *E*. Both charging and vehicle to grid (V2G) operating modes are simulated. Symmetrical six-phase induction machine parameters, used in the simulation, are the following: $R_s = R_r = 3\Omega$, $L_{\gamma s}$ =5mH, $L_{\gamma r}$ = 5mH, L_m = 185mH, two pole pairs, $J = 0.1\text{kgm}^2$.

A. Charging Mode

Ideal voltage source of the battery for the charging mode is *E*=597V. However, for the V2G mode (next subsection) a different value is considered. This is justified by the existence of a dc-dc converter between the battery and the converter in the real-world system (omitted here), so that the dc-bus voltage can be adjustable to various grid standards. The reference value for the dc-bus voltage is set to 600V.

Fig. 4a depicts grid phase voltage and current. It can be seen that the grid current is in phase with the voltage, demonstrating the unity power factor operation. It has a relatively high ripple due to the small leakage inductance of the machine, which was chosen to have a realistic value.

Grid current spectrum is given in Fig. 4b and it contains only small low order harmonics. Grid current components are depicted in Fig. 4c. Only the *d*-axis current component has a non-zero value. The *q*, *x* and *y* components are controlled to zero. It is clear that the charging process utilizes only the component that is in phase with the grid voltage, ensuring the unity power factor operation.

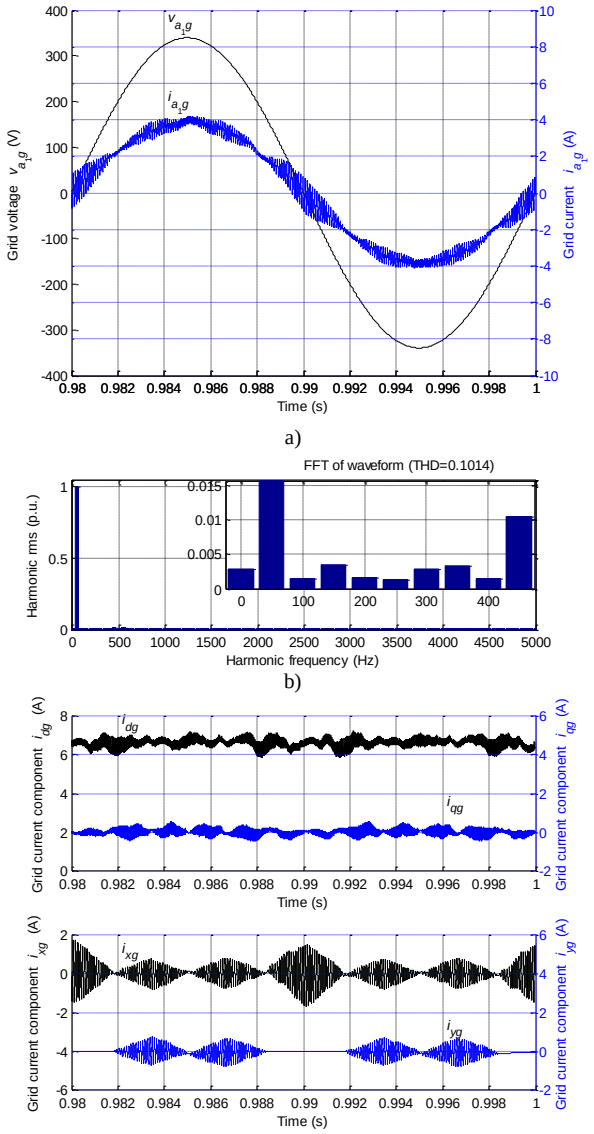

Fig. 4. Charging mode: (a) Grid phase voltage and current, (b) grid current spectrum, (c) grid current components.

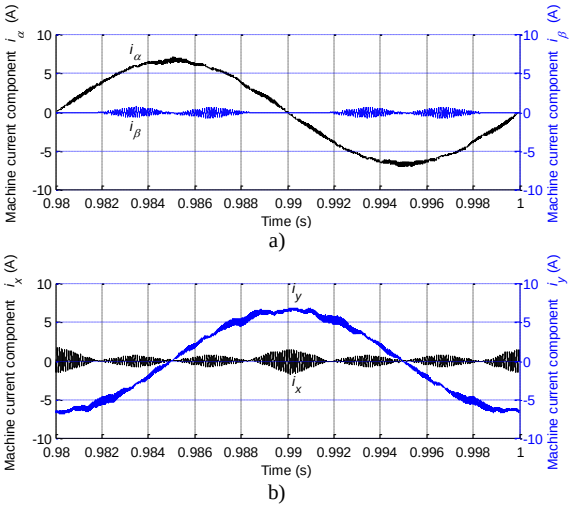

Fig. 5. Machine's current components: (a) i_α and i_β, (b) i_x and i_y.

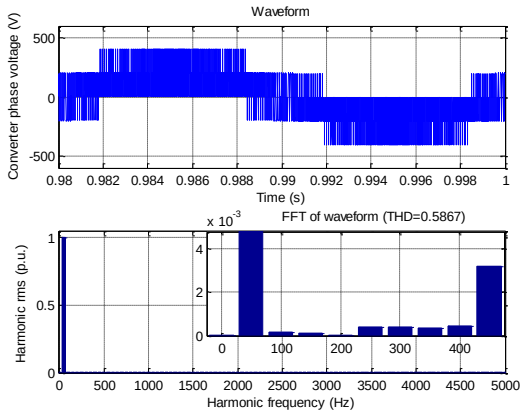

Fig. 6. Converter phase voltage and spectrum.

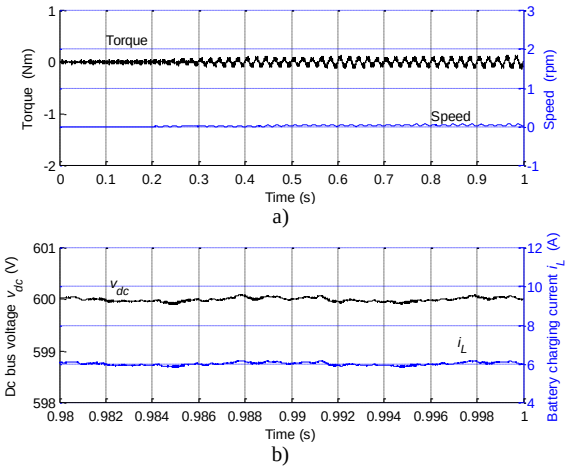

Fig. 7. (a) Machine's torque and speed, (b) dc-bus voltage and charging current.

Machine's phase current is the same as the grid phase current presented in Fig. 4a. However, its current components are different than the grid components, and they are now presented in Fig. 5. The first plane is not without excitation - Fig. 5a. Nevertheless, only single component (α) exists, which produces a pulsating field in the machine that is not capable of producing the average torque. The charging process utilises both planes, but only two components (α and y) are used, as was predicted in (4) and (5).

Converter phase voltage is shown in Fig. 6 and, due to the neglected dead time, it in essence does not contain low order harmonics. Fig. 7a shows that torque has zero average value, and that the speed stays at zero, with negligible oscillations. Fig. 7b shows that the dc-bus voltage is controlled to 600V, and that the charging current is, as expected, of the same shape as the voltage.

B. V2G Mode of the Symmetrical Six-phase System

The capability of the topology to inject the electric energy into the grid is demonstrated in this sub-section. As noted, the bidirectional dc-dc converter was not considered, but its existence is assumed between the battery and the VSR, so that the battery can be represented with an ideal voltage of E = 633V, and a resistor of R_L=0.5Ω. The dc-bus voltage reference is set to 630V.

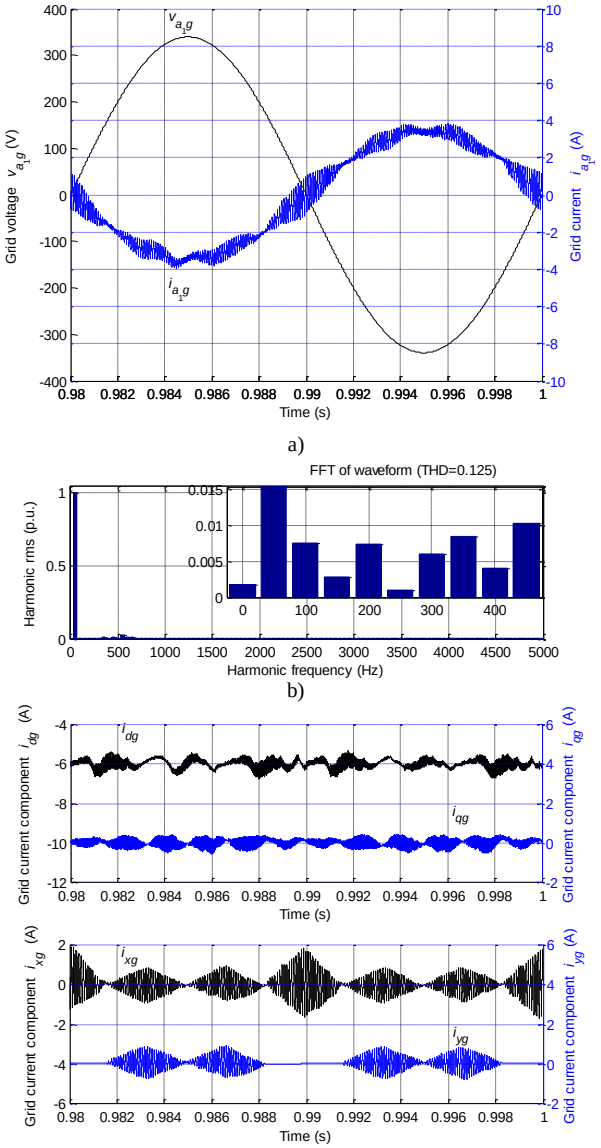

Fig. 8. V2G mode: (a) Grid phase voltage and current, (b) grid current spectrum, (c) grid current components.

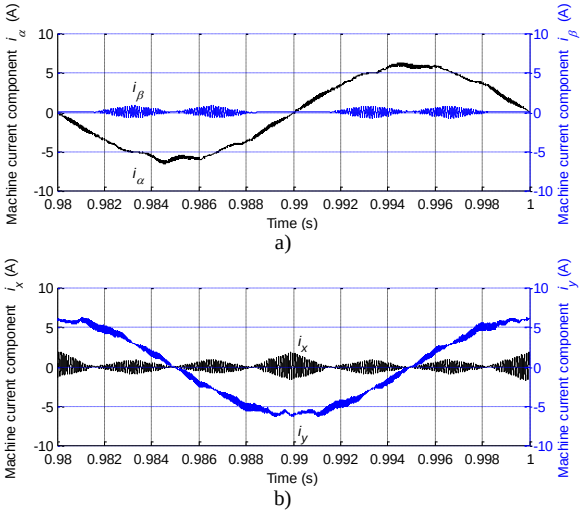

Fig. 9. Machine's current components: (a) i_α and i_β, (b) i_x and i_y.

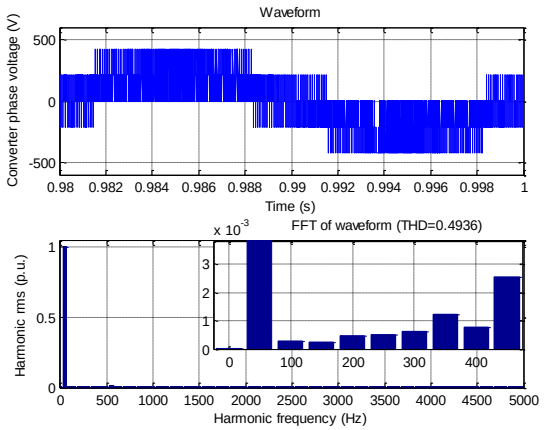

Fig. 10. Converter phase voltage and spectrum.

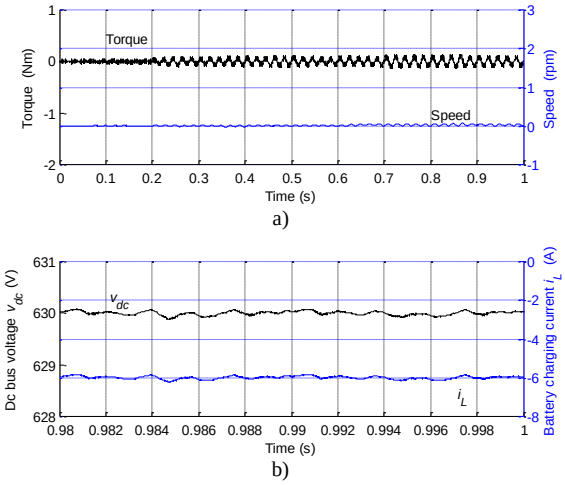

Fig. 11. (a) Machine's torque and speed, (b) dc-bus voltage and charging current.

As it was stated in the previous section, the control is the same for both charging and V2G modes. The only difference is that for V2G mode the reference voltage has to be lower than the battery voltage. Dc-bus voltage has to be higher than in the charging mode, to be able to produce a voltage that is higher than the first harmonic of the grid phase voltage by a value of the voltage drop on the machine windings. This voltage drop increases linearly with the transferred power.

Fig. 8 shows the grid voltage and current, current spectrum and its axis components. As can be seen, the current is in counter-phase with the voltage, which shows that the energy is injected into the grid with the unity power factor. It has negligible low order harmonics. All the current components are kept at zero except the *d*-axis component, which now has the opposite (negative) sign.

Machine's current components are presented in Fig. 9. The power is again transferred through both planes, but using only one of two components in each plane. Excited components have opposite signs, when compared to the charging mode of operation (Fig. 5).

Converter phase voltage contains negligible low order harmonics (Fig. 10). Torque and speed are again kept at zero (Fig. 11a), thus the rotor does not have to be mechanically locked during this mode of operation either. Dc-bus voltage is controlled at 630V. The dc current has the same value as for the charging mode of operation, but the sign is opposite (Fig. 11b), which agrees with the power flow direction.

V. Conclusion

A symmetrical six-phase machine with two isolated neutral points and a six-phase inverter is considered for integration into the EVs' charging process in the paper. It is shown how additional degrees of freedom of the machine can be conveniently utilized to avoid torque production in the machine, although charging currents flow through its stator windings. Simulations with a full model of the symmetrical six-phase machine are performed both for the charging and V2G modes in order to validate theoretical results.

Acknowledgement

The authors would like to acknowledge the Engineering and Physical Sciences Research Council (EPSRC) for supporting the Vehicle Electrical Systems Integration (VESI) project (EP/I038543/1).

References

[1] J. de Santiago, H. Bernhoff, B. Ekergård, S. Eriksson, S. Ferhatovic, R. Waters, and M. Leijon, "Electrical motor drivelines in commercial all-electric vehicles: A review," *IEEE Trans. on Vehicular Technology*, vol. 61, no. 2, pp. 475-484, 2012.

[2] S. Kinoshita, "Electric system of electric vehicle," *US Patent* No. 5,629,603, 1997.

[3] F. Lacressonniere and B. Cassoret, "Converter used as a battery charger and a motor speed controller in an industrial truck," *Proc. Eur. Conf. on Power Electr. and Applications EPE*, Dresden, Germany, CD-ROM paper 0159, 2005.

[4] S. Haghbin, S. Lundmark, M. Alakula, and O. Carlson, "An isolated high-power integrated charger in electrified-vehicle applications," *IEEE Trans. on Vehicular Technology*, vol. 60, no. 9, pp. 4115-4126, 2011.

[5] I. Subotic, E. Levi, M. Jones, and D. Graovac, "Multiphase integrated on-board battery chargers for electrical vehicles," *Proc. European Power Electronics and Applications Conf. EPE*, Lille, France, CD-ROM paper 0304, 2013.

[6] L. De Sousa, B. Silvestre, and B. Bouchez, "A combined multiphase electric drive and fast battery charger for electric vehicles," *Proc. IEEE Vehicle Power and Propulsion Conference VPPC*, Lille, France, CD-ROM, 2010.

[7] I. Subotic, E. Levi, M. Jones, and D. Graovac, "On-board integrated battery chargers for electric vehicles using nine-phase machines," *IEEE Int. Electric Machines and Drives Conf. IEMDC*, Chicago, IL, pp. 239-246, 2013.

[8] Renault press kit, "Renault ZOE: the electric supermini for everyday use," www.media.renault.com, February 26, 2013.

[9] I. Subotic, E. Levi, M. Jones, and D. Graovac, "An integrated battery charger for EVs based on an asymmetrical six-phase machine," *IEEE Industrial Electronics Society Conf. IECON*, Vienna, Austria, pp. 7242-7247, 2013

[10] E. Levi, M. Jones, S.N. Vukosavic, and H.A. Toliyat, "A novel concept of a multiphase, multimotor vector controlled drive system supplied from a single voltage source inverter," *IEEE Trans. on Power Electronics*, vol. 19, no. 2, pp. 320- 335, 2004.

[11] E. Levi, R. Bojoi, F. Profumo, H.A. Toliyat, and S. Williamson, "Multiphase induction motor drives - a technology status review," *IET Electric Power Applications*, vol. 1, no. 4, pp. 489-516, 2007.

[12] E. Levi, S.N. Vukosavic, and M. Jones, "Vector control schemes for series-connected six-phase two-motor drive systems", *IEE Proc. – Electric Power Applications*, vol. 152, no. 2, pp. 226-238, 2005.

[13] M. Jasinski and M.P. Kazmierkowski, "Fundamentals of ac-dc-ac converters control and applications," in *The Industrial Electronics Handbook – Power Electronics and Motor Drives* (Chapter 16), edited by B.M. Willamowski and J.D. Irwin, CRC Press, 2011.